Phonon Inverse Faraday Effect from Electron-Phonon Coupling

Phonon Inverse Faraday Effect from Electron-Phonon Coupling

Natalia Shabala* and R. Matthias Geilhufe†
Department of Physics, Chalmers University of Technology, 412 96 Göteborg, Sweden

(Received 12 July 2024; accepted 22 November 2024; published 26 December 2024)

The phonon inverse Faraday effect describes the emergence of a dc magnetization due to circularly polarized phonons. In this work we present a microscopic formalism for the phonon inverse Faraday effect. The formalism is based on time-dependent second order perturbation theory and electron phonon coupling. While our final equation is general and material independent, we provide estimates for the effective magnetic field expected for the ferroelectric soft mode in the oxide perovskite $SrTiO_3$. Our estimates are consistent with recent experiments showing a huge magnetization after a coherent excitation of circularly polarized phonons with THz laser light. Hence, the theoretical approach presented here is promising for shedding light into the microscopic mechanism of angular momentum transfer between ionic and electronic angular momentum, which is expected to play a central role in the phononic manipulation of magnetism.

DOI: 10.1103/PhysRevLett.133.266702

Introduction—Circularly polarized phonons or axial phonons are lattice vibrations with a nonzero angular momentum. These lattice vibrations can induce a magnetization in the material. This magnetization is an example of dynamical multiferroicity, the phenomenon in which the motion of ions in a crystal causes its polarization to vary in time, thus inducing a net magnetization [1–4].

While the gyromagnetic ratio of the phonon hints towards a magnetization in the order of the nuclear magneton, recent experiments using phonon Zeeman effect and magneto-optical Kerr effect [5–10] show that the size of the magnetization resulting from circularly polarized moment is quite significant, with magnetic moments on the order of magnitude of $0.1-10\mu_B$. This is a promising route for using phonons for magnetic manipulation [11], as has recently been shown on the example of the magnetic switching due to the ultrafast Barnett effect [12]. Here, the Barnett effect [13] describes the magnetization of a nominally nonmagnetic sample due to mechanical rotation, and is the inverse of the so-called Einstein–de-Haas effect [14]. Recently, both effects have been brought into the characteristic timescales and length scales of material excitations, and phenomenologically describe the angular momentum transfer between magnetization and phonons [12,15,16].

These findings call for a microscopic theory of angular momentum transfer between phonons and electrons for describing the phonon-induced magnetic moments. As a result, multiple microscopic theories of this have been proposed, explaining the size of the phonon-induced magnetic moment, e.g., by inertial effects [17,18], orbit-lattice coupling [19], spin-orbit coupling [20], orbital magnetization [21], electron-nuclear quantum geometry [22], non-Maxwellian fields [23,24]. While these approaches show similarities and overlap in their formalism, the consensus on the microscopic theory behind the effect has not yet been reached.

In contrast, the optical analog, i.e., the transfer of spin angular momentum from circularly polarized light to electron spin is well-described by the inverse Faraday effect [25]. Here, the electric field of the light couples to the electron via the dipole-interaction. From a symmetry perspective, the concept of inverse Faraday effect is universal and can be generalized to any circularly polarized vector field, beyond a laser field. Examples comprise axial magnetoelectric effect [26] and the *phonon inverse Faraday effect* [11]. Here, we provide the microscopic theory for the phonon inverse Faraday effect by coupling circularly polarized phonons to electrons via the electron-phonon interaction.

Phonon inverse Faraday effect: Phenomenological theory—We start with a phenomenological description of the phonon inverse Faraday effect, similar to Pershan *et al.* [25] and the optical inverse Faraday effect. For simplicity, we consider twofold degenerate phonon level, with two modes u_μ and u_ν. We are free to introduce a basis transform, e.g., to the circularly polarized basis,

$$\boldsymbol{u}(t) = \left(\frac{1}{\sqrt{2}} u_R(\hat{\boldsymbol{e}}_\mu + i\hat{\boldsymbol{e}}_\nu) + \frac{1}{\sqrt{2}} u_L(\hat{\boldsymbol{e}}_\mu - i\hat{\boldsymbol{e}}_\nu)\right) e^{i\omega t}, \quad (1)$$

with $u_R = (u_\mu - iu_\nu)/\sqrt{2}$ and $u_L = (u_\mu + iu_\nu)/\sqrt{2}$. We need to define free energy function in terms of phonon

*Contact author: natalia.shabala@chalmers.se
†Contact author: matthias.geilhufe@chalmers.se

mode amplitudes. To fulfill the symmetry criteria of a nonmagnetic and inversion symmetric crystal, the thermodynamic free energy has to be invariant under time reversal and space inversion. This gives rise to the following phenomenological coupling between circularly polarized phonons and the magnetic field $\boldsymbol{H}$,

$$F_u = \chi H_z (u_R u_R^* - u_L u_L^*) = i\chi H_z (u_\mu u_\nu^* - u_\nu u_\mu^*). \quad (2)$$

As a result, the magnetization is given by

$$M_z = -\frac{\partial F_u}{\partial H_z} = \chi \left(u_L u_L^* - u_R u_R^*\right). \quad (3)$$

From the equation above it becomes evident that an imbalance of circularly polarized phonons induce the dc magnetization of the material. Such an imbalance can be induced by coherent excitation with circularly polarized laser light [5,6,12]. However, the effect itself is purely phononic and does not require light. To offer a full picture, we give the phononic Faraday rotation,

$$\Delta\epsilon_R^u = -4\pi \frac{\partial^2 F_u}{\partial u_R \partial u_R^*} = -4\pi\chi H_z, \quad (4)$$

$$\Delta\epsilon_L^u = -4\pi \frac{\partial^2 F_u}{\partial u_L \partial u_L^*} = 4\pi\chi H_z, \quad (5)$$

where $\epsilon_{R,L}^u$ denote a phonon response function, i.e., the response of the medium to a phonon mode. $\epsilon_{R,L}^u$ can be understood by analogy with dielectric constant ϵ. Optical Faraday rotation can be described as a change of the dielectric constant in the presence of an applied magnetic field: $\Delta\epsilon_{R,L} = -4\pi(\partial^2 F_E/\partial E_R \partial E_R^*) = -4\pi\chi H_z$ [25]. This change induces a rotation of polarization of linearly polarized light beam passing through the medium. In case of phonon Faraday rotation the change of the phonon response function causes a rotation of polarization direction of a linearly polarized phonon mode in the presence of an applied magnetic field.

Here we presented a simple phenomenological theory that explains the emergence of magnetization from circularly polarized phonons. However, this approach does not allow us to simply estimate the size of the resulting magnetization since the material constant χ remains unknown. In the sections below we present a microscopic theory that addresses this problem.

Phonon inverse Faraday effect: Microscopical theory—In the following we develop the microscopic theory of the phonon inverse Faraday effect. A phonon is the collective excitation of the lattice, i.e., time-dependent displacements of the ions around their equilibrium positions. Hence, phonons introduce a time-dependent perturbation $V(t)$ into the system, $\hat{H} = \hat{H}_0 + V(t)$. We assume that the atom displacements $u_{pj\alpha}$ are sufficiently small and the potential function can be written as a first-order Taylor expansion. Then the perturbation $V(t)$ is given by

$$V(t) = \sum_{pj\alpha} \frac{\partial U}{\partial u_{pj\alpha}} u_{pj\alpha}, \quad (6)$$

where we consider the variation of the potential due to displacement of atom j in Cartesian direction α in a unit cell p.

Before presenting the main result, we outline our approach for a single ion with displacement $\boldsymbol{u}(t)$. To allow for circular polarization, $\boldsymbol{u}(t)$ is generally complex. In this case the real-valued perturbation becomes $V(t) = 2\Re[\boldsymbol{u}(t) \cdot \nabla_{\boldsymbol{u}} U]$. Hence, we express the time-dependent perturbation as follows,

$$V(t) = v e^{i\omega t} + v^* e^{-i\omega t}, \quad (7)$$

where ω denotes the phonon frequency. Equation (7) gives rise to an effective Hamiltonian in second order perturbation theory [25],

$$\langle a|H_{\text{eff}}(t)|b\rangle = -\sum_n \left[\frac{\langle a|v|n\rangle\langle n|v^*|b\rangle}{E_{nb} - \hbar\omega} - \frac{\langle a|v^*|n\rangle\langle n|v|b\rangle}{E_{nb} + \hbar\omega}\right]. \quad (8)$$

Here, $|n\rangle$ are eigenstates of the unperturbed Hamiltonian, and $E_{nb} = E_n - E_b$ denotes the energy difference between states $|n\rangle$ and $|b\rangle$. We evaluate the effective Hamiltonian (8) and only keep terms giving a contribution to the magnetization as discussed in (3). This allows us to formulate the following revised effective Hamiltonian,

$$\mathcal{H}_{\text{eff}}^{ab}(\boldsymbol{k}) = -\hbar\omega(\boldsymbol{u} \times \boldsymbol{u}^*)_z \times \sum_n \frac{(\langle a|\nabla U|n\rangle \times \langle n|\nabla U|b\rangle)_z}{E_{\boldsymbol{k}nb}^2 - \hbar^2\omega^2}. \quad (9)$$

Equation (9) represents a semiclassical solution where the ionic displacement is not quantized. We generalize the single ion case for the entire crystal by introducing quantized normal coordinates for phonon modes μ and ν:

$$u_{p\mu} = i\sum_{\boldsymbol{q}} e^{i\boldsymbol{q}\cdot\boldsymbol{R}_p} l_{\boldsymbol{q}\mu}\left(\hat{a}_{\boldsymbol{q}\mu} + \hat{a}_{-\boldsymbol{q}\mu}^\dagger\right),$$
$$u_{p\nu} = \sum_{\boldsymbol{q}} e^{i\boldsymbol{q}\cdot\boldsymbol{R}_p} l_{\boldsymbol{q}\nu}\left(\hat{a}_{\boldsymbol{q}\nu} + \hat{a}_{-\boldsymbol{q}\nu}^\dagger\right). \quad (10)$$

Here, $l_{\boldsymbol{q}\nu} = \sqrt{(\hbar/2\omega_{\boldsymbol{q}\nu})}$ is the zero displacement amplitude. Operators $\hat{a}_{\boldsymbol{q}\nu}^\dagger$ and $\hat{a}_{\boldsymbol{q}\nu}$ are bosonic creation and annihilation operators. Together the phonon modes (10) form a circularly polarized phonon mode according to Eq. (1).

To describe the electron-phonon coupling we introduce electron-phonon matrix elements $g_{mn\nu}(\boldsymbol{k}, \boldsymbol{q})$ which describe the probability amplitude of an electron absorbing a phonon of mode ν and wave vector $\boldsymbol{q}$ and scattering from

state $|n,\boldsymbol{k}\rangle$ to state $|m,\boldsymbol{k}+\boldsymbol{q}\rangle$ [27,28]. A schematic diagram is given in Fig. 1(b). Following Ref. [28], the electron-phonon matrix elements are given by

$$g_{mn\nu}(\boldsymbol{k},\boldsymbol{q}) = \langle m,\boldsymbol{k}+\boldsymbol{q}|\sum_p l_{\boldsymbol{q}\nu} e^{i\boldsymbol{q}\cdot\boldsymbol{R}_p}\frac{\partial U}{\partial u_{p\nu}}|n,\boldsymbol{k}\rangle. \tag{11}$$

Using Eqs. (10) and (11), we extend the single ion effective Hamiltonian (9) and obtain the following effective Hamiltonian for the entire crystal,

$$\mathcal{H}^{ab}_{\mathrm{eff}}(\boldsymbol{k}) = -i\hbar\omega\sum_{\boldsymbol{q}}\left[\left(\hat{a}_{\boldsymbol{q},\mu}+\hat{a}^{\dagger}_{-\boldsymbol{q},\mu}\right)\left(\hat{a}^{\dagger}_{-\boldsymbol{q},\nu}+\hat{a}_{\boldsymbol{q},\nu}\right)\sum_n \frac{g_{an\mu}(\boldsymbol{k},\boldsymbol{q})g^{*}_{bn\nu}(\boldsymbol{k},\boldsymbol{q}) - g_{an\nu}(\boldsymbol{k},\boldsymbol{q})g^{*}_{bn\mu}(\boldsymbol{k},\boldsymbol{q})}{E^2_{\boldsymbol{k}nb}-\hbar^2\omega^2}\right]. \tag{12}$$

We note that Eq. (12) makes no assumptions on the material and represents the main theoretical result of our Letter.

Furthermore, we can show that (12) can be connected to the phonon number operator. We introduce operators $\hat{a}_{\boldsymbol{q}}$, $\hat{a}^{\dagger}_{-\boldsymbol{q}}$, such that $\boldsymbol{\epsilon}\hat{a}_{\boldsymbol{q}} = \begin{pmatrix}\hat{a}_{\boldsymbol{q},\mu}\\ \hat{a}_{\boldsymbol{q},\nu}\end{pmatrix}$, $\boldsymbol{\epsilon}^{*}\hat{a}^{\dagger}_{-\boldsymbol{q}} = \begin{pmatrix}\hat{a}^{\dagger}_{-\boldsymbol{q},\mu}\\ \hat{a}^{\dagger}_{-\boldsymbol{q},\nu}\end{pmatrix}$. Now, using bosonic anticommutation relations, we can reformulate (12) as

$$\mathcal{H}^{ab}_{\mathrm{eff}}(\boldsymbol{k}) = -2i\hbar\omega\sum_{\boldsymbol{q}}\left[\left(\hat{a}^{\dagger}_{-\boldsymbol{q}}\hat{a}_{\boldsymbol{q}}+\frac{1}{2}\delta_{-\boldsymbol{q},\boldsymbol{q}}\right)\sum_n \frac{g_{an\mu}(\boldsymbol{k},\boldsymbol{q})g^{*}_{bn\nu}(\boldsymbol{k},\boldsymbol{q}) - g_{an\nu}(\boldsymbol{k},\boldsymbol{q})g^{*}_{bn\mu}(\boldsymbol{k},\boldsymbol{q})}{E^2_{\boldsymbol{k}nb}-\hbar^2\omega^2}\right], \tag{13}$$

where, following Zhang and Niu [15], we have omitted $\hat{a}_{\boldsymbol{q}}\hat{a}_{\boldsymbol{q}}$ and $\hat{a}^{\dagger}_{-\boldsymbol{q}}\hat{a}^{\dagger}_{-\boldsymbol{q}}$ terms. Additionally, we have used polarization vector property $\varepsilon^{*}_{\mu}\varepsilon_{\nu} = \delta_{\mu\nu}$, and the fact that for degenerate phonon modes that equally contribute to a circularly polarized mode we can set $\varepsilon_{\mu} = \varepsilon_{\nu}$. For a soft mode at Γ point $\hat{a}^{\dagger}_{-\boldsymbol{q}}\hat{a}_{\boldsymbol{q}}$ becomes $\hat{n}_{\boldsymbol{0}} = \hat{a}^{\dagger}_{\boldsymbol{0}}\hat{a}_{\boldsymbol{0}}$, which is the occupation number operator for circularly polarized phonon mode at the Γ point.

Relating to the recent finding of the large dynamical multiferroicity in $SrTiO_3$ [5] we discuss the effective Hamiltonian (12) for cubic symmetry and an infrared active optical phonon mode with T_{1u} symmetry. The electronic structure of $SrTiO_3$ is schematically shown in Fig. 2. The valence band is primarily composed of oxygen p states (T_{1u}) and the conduction band is composed of Ti-d states (T_{2g}). To estimate the effective magnetic field imposed on the electrons by axial phonons, we discuss the level splitting of Γ-point states transforming as $p_{\pm} = (p_x \pm ip_y)/\sqrt{2}$. Hence, we evaluate the overlap elements $\mathcal{H}^{xy}_{\mathrm{eff}}(\boldsymbol{0})$ and $\mathcal{H}^{yx}_{\mathrm{eff}}(\boldsymbol{0})$ in the effective Hamiltonian (12). Here, we use two assumptions. First, the electron-phonon coupling elements $g_{an\nu}$ are subject to selection rules [29,30]. As both, the phonon mode and the p orbitals are parity-odd, the overlap needs to involve parity-even orbitals, i.e., the Ti-d states [31,32] (details given in the Supplemental Material [33]). Second the perturbative sum in (12) rapidly decreases with the spectral distance, $\mathcal{H}^{ab}_{\mathrm{eff}} \sim E^{-2}_{nb}$ for $E_{nb} \gg \hbar\omega$. Using these assumptions and cubic symmetry, we derive (details given in the Supplemental Material [33]),

$$\mathcal{H}^{xy}_{\mathrm{eff}}(\boldsymbol{0}) = -\mathcal{H}^{yx}_{\mathrm{eff}}(\boldsymbol{0}), \tag{14}$$

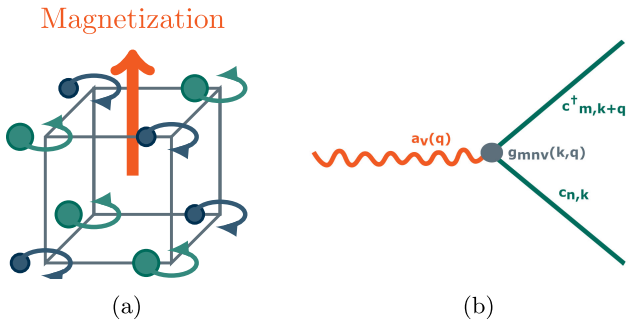

FIG. 1. (a) Schematically depicted phonon inverse Faraday effect. (b) Vortex diagram of electron-phonon interaction: electron in a state $|n,\boldsymbol{k}\rangle$ absorbs a phonon of mode ν with a wave vector $\boldsymbol{q}$ and scatters to a state $|m,\boldsymbol{k}+\boldsymbol{q}\rangle$.

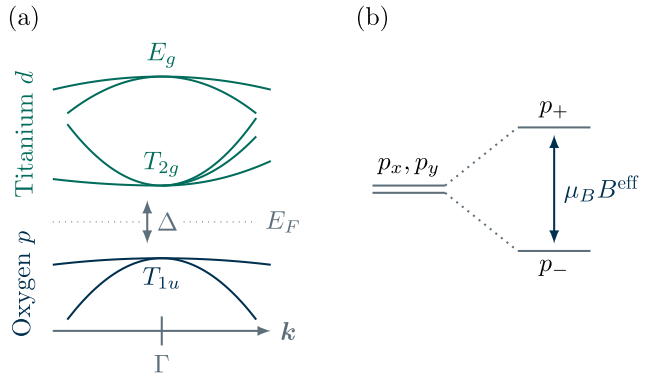

FIG. 2. Schematic of the electronic structure of $SrTiO_3$. (a) Orbital character of valence and conduction bands. (b) Splitting of p orbitals in the effective magnetic field.

$$\mathcal{H}^{xy}_{\mathrm{eff}}(\mathbf{0}) = -i\left(\hat{n}_{\mathbf{0}} + \frac{1}{2}\right)\frac{\hbar\omega|g|^2}{\Delta^2 - \hbar^2\omega^2}. \tag{15}$$

A basis transform to $p_\pm = (p_x \pm ip_y)/\sqrt{2}$, i.e., $H^{\pm\pm}_{\mathrm{eff}} = \pm i\mathcal{H}^{xy}_{\mathrm{eff}}$ gives a two-phonon amplitude

$$E^{\pm} = \pm\frac{\hbar\omega|g|^2}{\Delta^2 - \hbar^2\omega^2}\left(n_{\mathbf{0}} + \frac{1}{2}\right). \tag{16}$$

At room temperature, the infrared-active ferroelectric soft-mode in $SrTiO_3$ has a frequency of 2.7 THz [5,34], i.e., $\hbar\omega \approx 11$ meV. In contrast, the measured direct band gap of $SrTiO_3$ is $\Delta \approx 3.75$ eV [35]. If we assume an electron phonon coupling of $g \approx 7$ meV [36,37], we obtain $\Delta E = E^+ - E^- \approx 7.7 \times 10^{-8}(n_{\mathbf{0}} + \frac{1}{2})$ eV. If we compare this to the expected Zeeman splitting due to a magnetic field,

$$\frac{\Delta E}{2} = g_J\mu_B B^{\mathrm{eff}}_z, \tag{17}$$

we can estimate the effective magnetic field for $J = 1$. Relating to the measurements done on $SrTiO_3$ [5], we first estimate the number of phonons resulting from the pump field strength of $E_0 = 230$ kV/cm that was used in the experiment. The maximal peak intensity of laser field is given by $I_{\max} = (1/2\mu_0 c)\tilde{E}_0^2$, where $\tilde{E}_0 = \beta E_0$ is the electric field strength in the material. In our calculations we assume the screening constant $\beta = 0.7$, in agreement with Ref. [5]. With the energy of a single photon, we can estimate the number of incident photons per area of a unit cell as $N \approx 30$ 1/ps. Given a pulse width of 2 ps, that results in the total number of incident photons per unit cell area $N^{\mathrm{ph}} = 60$. At the same time, at the resonance frequency we can assume that one photon is able to excite one phonon. Therefore $N^{\mathrm{ph}} \approx 60$ will excite 60 phonons at the surface, i.e., $n_{\mathbf{0}} = 60$. Thus, from (17) we can estimate the effective magnetic field to be $B^{\mathrm{eff}} \approx 40$ mT. Basini *et al.* [5] report an effective magnetic field of 32 mT at the surface of the sample, therefore we can conclude that our estimate is in agreement with the experimental observations. Here we also want to highlight that since the number of phonons is proportional to the laser intensity, $n_{\mathbf{0}} \propto I$, the magnitude of the effect scales with the square of the pump's electric field strength, E_0^2, which is a characteristic signature of the effect.

We stress that the effective magnetic field is not a "physical" magnetic field as described by Maxwell's equations. Still, it provides a time-reversal symmetry breaking field. Recently, Merlin [23] pointed out that by probing a material with the magneto-optical Kerr effect, such a time-reversal symmetry breaking field, or non-Maxwellian field, leads to a Kerr rotation of the linearly polarized probe laser, with electric field $\boldsymbol{\varepsilon}$. This process can be described phenomenologically by the following free energy

$$F_{\mathrm{MOKE}} = i\Lambda B^{\mathrm{eff}}(\boldsymbol{\varepsilon} \times \boldsymbol{\varepsilon}^*), \tag{18}$$

where the Kerr rotation results from the difference of the dielectric constants for left- and right-circularly polarized light, in the presence of circularly polarized phonons and a resulting effective magnetic field,

$$\Delta\epsilon_R = -4\pi\Lambda B^{\mathrm{eff}}, \qquad \Delta\epsilon_L = 4\pi\Lambda B^{\mathrm{eff}}. \tag{19}$$

Equation (19) follows a similar derivation as shown in Eq. (5) [25].

In the experiment reported by Basini *et al.* [5], circularly polarized phonons in $SrTiO_3$ were induced by a circularly polarized laser field. Because of screening in the material, the penetration depth of the laser pump pulse, measured by the decay length l_{decay} is in the order of $l_{\mathrm{decay}} \approx 2.5$ μm. Hence, the expected Faraday rotation can be estimated as follows [5,38]:

$$\theta_F = \frac{l_{\mathrm{decay}}V}{2}B^{\mathrm{eff}}_z \tag{20}$$

$$= \frac{l_{\mathrm{decay}}V}{2}\frac{1}{\mu_B}\frac{\hbar\omega|g|^2}{\Delta^2 - \hbar^2\omega^2}\left(n_{\mathbf{0}} + \frac{1}{2}\right). \tag{21}$$

Here, V is the Verdet constant of the material, which is $V \approx 180$ rad m^{-1} T^{-1} for $SrTiO_3$ [5].

Since Kerr and Faraday rotation are closely related and are not different by more than a factor of 2 in $SrTiO_3$ [5], an estimate of Faraday rotation gives a good picture approximation of Kerr rotation resulting from the same magnetic field. In Fig. 3 we plot Faraday rotation calculated using (20) as a function of electric field strength E_0. Comparison

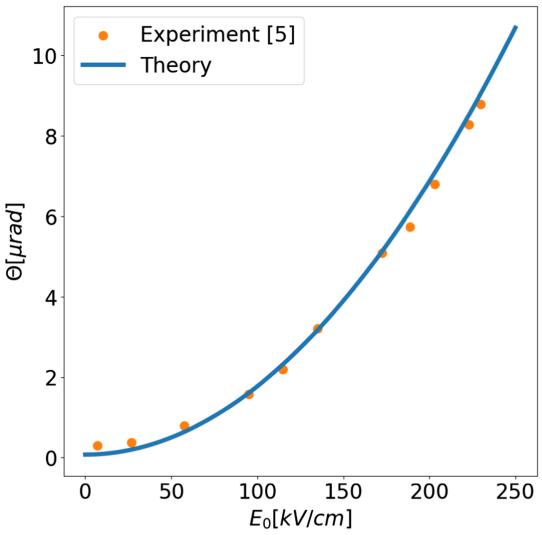

FIG. 3. Polarization rotation as a function of electric field strength. Solid line is the Faraday rotation obtained with (20) and $|g| = 7$ meV. Dots represent Kerr rotation measurements reported by Basini *et al.* [5].

to experimental measurements of Kerr rotation [5] shows that for $|g| = 7$ meV our estimate is in perfect agreement with the experimental values. Here we would like to emphasize again that our plot shows a quadratic dependency of the effect on the electric field strength.

Discussion and summary—To highlight the fact that phonon inverse Faraday effect arises from circularly polarized phonons, we consider the ladder operators $(\hat{a}_{\mathbf{0},\mu} + \hat{a}^{\dagger}_{\mathbf{0},\mu})(\hat{a}^{\dagger}_{\mathbf{0},\nu} + \hat{a}_{\mathbf{0},\nu})$ in the effective Hamiltonian (15), and define $\hat{O}_{\mu} = \hat{a}_{\mathbf{0},\mu} + \hat{a}^{\dagger}_{\mathbf{0},\mu}$ and $\hat{O}_{\nu} = \hat{a}_{\mathbf{0},\nu} + \hat{a}^{\dagger}_{\mathbf{0},\nu}$, respectively. These operators describe the amplitude of the corresponding phonon modes μ and ν. Similarly to Ref. [19], we introduce operators $\hat{O}_{\pm} = (\hat{O}_{\mu} \pm i\hat{O}_{\nu})/\sqrt{2}$, which allows us to write the effective Hamiltonian (15) as

$$\mathcal{H}^{\pm\pm}_{\mathrm{eff}}(\mathbf{0}) = \mp \frac{i}{4}\left(\hat{O}_{+}\hat{O}_{+} - \hat{O}_{-}\hat{O}_{-}\right)\frac{\hbar\omega|g|^2}{\Delta^2 - \hbar^2\omega^2}. \tag{22}$$

Finally, we would like to relate our result to other theories on the problem. We note that Eq. (12) is a generalization of the orbit-lattice coupling described by Chaudhary *et al.* [19]. In the $4f$ paramagnets such as $CeCl_3$, the spectral distance E_{nb} is dominated by either spin-orbit interaction ($\approx$0.1 eV) or by the crystal field splitting (6 meV). As a result, the expected effective magnetic field is significantly larger as compared to $SrTiO_3$. In fact, this is consistent with experimental work [6,10] as well as theoretical estimates [19,39]. The argument of tiny spectral gaps due to crystal field effects is also found in connection to a dynamical crystal field effect imposed by the phonon [22]. Furthermore, for materials with large gap $\Delta \gg \hbar\omega$, the denominator of the effective magnetic field becomes independent of the phonon frequency, i.e., $\Delta^2 - \hbar^2\omega^2 \approx \Delta^2$. In this limit, the level splitting is linearly dependent of the phonon frequency, $\Delta E \sim \hbar\omega$, which is related to the inertial effects discussed in Refs. [17,18]. The same strong suppression of the expected effective magnetic field or magnetization by the band gap, $B^{\mathrm{eff}} \sim \Delta^{-2}$, found in the present work, is also revealed in the formalism of the modern theory of magnetization and the phonon magnetic moment from electronic topology [21,40]. In particular, in the adiabatic regime, Eq. (12) becomes identical to the formalism developed by Ren *et al.* [21].

In summary, the approach presented here provides a general and material-independent framework for estimating an emergent magnetization and effective magnetic field due to axial phonons, i.e., phonons carrying angular momentum [15]. As we discussed above, the advantage of the formalism that we present in this work lies in its generality. We have presented an estimate of the effective magnetic field resulting from circularly-polarized phonons for $SrTiO_3$, but using e.g. numerical methods Eq. (12) could be used in a similar way to estimate the effective magnetic field in other materials.

Moreover, the formalism presented here is strongly supported by the experimental evidence [5], as our results presented in Fig. 3 show. Furthermore, the result given by Eq. (12) highlights an important distinction between the phonon inverse Faraday effect and the optical inverse Faraday effect. While the microscopic theory of the optical inverse Faraday is based on the dipole coupling of the electric field to the electron, the phonon inverse Faraday effect is based on the electron-phonon interaction. As such the phonon inverse Faraday effect also occurs in the absence of a laser field, as long as an imbalance of left- and right-circularly polarized phonons is present. However, it is also worth noting that the circularly polarized phonons can be induced by a circularly polarized laser field [5]. Hence, for laser excitations resonant with phonons, both the phononic and the optical contribution coexist.

Note added—Recently, another interesting paper appeared discussing a similar approach [24].

Acknowledgments—We acknowledge inspiring discussions with Alexander Balatsky, Martina Basini, Stefano Bonetti, Dominik Juraschek, Finja Tietjen, Hanyu Zhu. We are grateful for support from the Swedish Research Council (VR starting Grant No. 2022-03350), the Olle Engkvist Foundation (Grant No. 229-0443), the Royal Physiographic Society in Lund (Horisont), the Knut and Alice Wallenberg Foundation (Grant No. 2023.0087), and Chalmers University of Technology, via the department of physics and the Areas of Advance Nano and Materials.

[1] Y. T. Rebane, Faraday effect produced in the residual ray region by the magnetic moment of an optical phonon in an ionic crystal, J. Exp. Theor. Phys. **84**, 2323 (1983), http://jetp.ras.ru/cgi-bin/e/index/e/57/6/p1356?a=list.

[2] D. M. Juraschek, M. Fechner, A. V. Balatsky, and N. A. Spaldin, Dynamical multiferroicity, Phys. Rev. Mater. **1**, 014401 (2017).

[3] D. M. Juraschek and N. A. Spaldin, Orbital magnetic moments of phonons, Phys. Rev. Mater. **3**, 064405 (2019).

[4] R. M. Geilhufe, V. Juričić, S. Bonetti, J.-X. Zhu, and A. V. Balatsky, Dynamically induced magnetism in $KTaO_3$, Phys. Rev. Res. **3**, L022011 (2021).

[5] M. Basini, M. Pancaldi, B. Wehinger, M. Udina, V. Unikandanunni, T. Tadano, M. C. Hoffmann, A. V. Balatsky, and S. Bonetti, Terahertz electric-field-driven dynamical multiferroicity in $SrTiO_3$, Nature (London) **628**, 534 (2024).

[6] J. Luo, T. Lin, J. Zhang, X. Chen, E. R. Blackert, R. Xu, B. I. Yakobson, and H. Zhu, Large effective magnetic fields from chiral phonons in rare-earth halides, Science **382**, 698 (2023).

[7] B. Cheng, T. Schumann, Y. Wang, X. Zhang, D. Barbalas, S. Stemmer, and N. Armitage, A large effective phonon magnetic moment in a Dirac semimetal, Nano Lett. **20**, 5991 (2020).

[8] A. Baydin, F. G. G. Hernandez, M. Rodriguez-Vega, A. K. Okazaki, F. Tay, G. T. Noe, I. Katayama, J. Takeda,

H. Nojiri, P. H. O. Rappl, E. Abramof, G. A. Fiete, and J. Kono, Magnetic control of soft chiral phonons in PbTe, Phys. Rev. Lett. **128**, 075901 (2022).
[9] F. G. G. Hernandez, A. Baydin, S. Chaudhary, F. Tay, I. Katayama, J. Takeda, H. Nojiri, A. K. Okazaki, P. H. O. Rappl, E. Abramof, M. Rodriguez-Vega, G. A. Fiete, and J. Kono, Observation of interplay between phonon chirality and electronic band topology, Sci. Adv. **9**, eadj4074 (2023).
[10] G. Schaack, Magnetic phonon splitting in rare earth trichlorides, Physica (Amsterdam) **89B+C**, 195 (1977).
[11] D. M. Juraschek, P. Narang, and N. A. Spaldin, Phono-magnetic analogs to opto-magnetic effects, Phys. Rev. Res. **2**, 043035 (2020).
[12] C. S. Davies, F. G. N. Fennema, A. Tsukamoto, I. Razdolski, A. V. Kimel, and A. Kirilyuk, Phononic switching of magnetization by the ultrafast Barnett effect, Nature (London) **628**, 540 (2024).
[13] S. J. Barnett, Magnetization by rotation, Phys. Rev. **6**, 239 (1915).
[14] A. Einstein, Experimenteller Nachweis der Ampéreschen Molekularströme, Die Naturwiss. **3**, 237 (1915).
[15] L. Zhang and Q. Niu, Angular momentum of phonons and the Einstein–de Haas effect, Phys. Rev. Lett. **112**, 085503 (2014).
[16] S. R. Tauchert, M. Volkov, D. Ehberger, D. Kazenwadel, M. Evers, H. Lange, A. Donges, A. Book, W. Kreuzpaintner, U. Nowak, and P. Baum, Polarized phonons carry angular momentum in ultrafast demagnetization, Nature (London) **602**, 73 (2022).
[17] R. M. Geilhufe, Dynamic electron-phonon and spin-phonon interactions due to inertia, Phys. Rev. Res. **4**, L012004 (2022).
[18] R. M. Geilhufe and W. Hergert, Electron magnetic moment of transient chiral phonons in $KTaO_3$, Phys. Rev. B **107**, L020406 (2023).
[19] S. Chaudhary, D. M. Juraschek, M. Rodriguez-Vega, and G. A. Fiete, Giant effective magnetic moments of chiral phonons from orbit-lattice coupling, Phys. Rev. B **110**, 094401 (2024).
[20] J. Fransson, Chiral phonon induced spin polarization, Phys. Rev. Res. **5**, L022039 (2023).
[21] Y. Ren, C. Xiao, D. Saparov, and Q. Niu, Phonon magnetic moment from electronic topological magnetization, Phys. Rev. Lett. **127**, 186403 (2021).
[22] L. Klebl, A. Schobert, G. Sangiovanni, A. V. Balatsky, and T. O. Wehling, Ultrafast pseudomagnetic fields from electron-nuclear quantum geometry, arXiv:2403.13070.
[23] R. Merlin, Unraveling the effect of circularly polarized light on reciprocal media: Breaking time reversal symmetry with non-Maxwellian magnetic-esque fields, Phys. Rev. B **110**, 094312 (2024).
[24] R. Merlin, Magnetophononics and the chiral phonon misnomer, arXiv:2404.19593.
[25] P. Pershan, J. Van der Ziel, and L. Malmstrom, Theoretical discussion of the inverse Faraday effect, Raman scattering, and related phenomena, Phys. Rev. **143**, 574 (1966).
[26] L. Liang, P. O. Sukhachov, and A. V. Balatsky, Axial magnetoelectric effect in Dirac semimetals, Phys. Rev. Lett. **126**, 247202 (2021).
[27] J.-J. Zhou, O. Hellman, and M. Bernardi, Electron-phonon scattering in the presence of soft modes and electron mobility in $SrTiO_3$ perovskite from first principles, Phys. Rev. Lett. **121**, 226603 (2018).
[28] F. Giustino, Electron-phonon interactions from first principles, Rev. Mod. Phys. **89**, 015003 (2017).
[29] L. Shu, Y. Xia, B. Li, L. Peng, H. Shao, Z. Wang, Y. Cen, H. Zhu, and H. Zhang, Full-landscape selection rules of electrons and phonons and temperature-induced effects in 2D silicon and germanium allotropes, npj Comput. Mater. **10**, 2 (2024).
[30] Y. Chen, Y. Wu, B. Hou, J. Cao, H. Shao, Y. Zhang, H. Mei, C. Ma, Z. Fang, H. Zhu, and H. Zhang, Renormalized thermoelectric figure of merit in a band-convergent Sb_2Te_2Se monolayer: Full electron–phonon interactions and selection rules, J. Mater. Chem. A **9**, 16108 (2021).
[31] W. Hergert and R. M. Geilhufe, *Group Theory in Solid State Physics and Photonics: Problem Solving with Mathematica* (Wiley-VCH, Weinheim, Germany, 2018), ISBN: 978-3-527-41133-7.
[32] R. M. Geilhufe and W. Hergert, GTPack: A Mathematica group theory package for application in solid-state physics and photonics, Front. Phys. **6**, 86 (2018).
[33] See Supplemental Material at http://link.aps.org/supplemental/10.1103/PhysRevLett.133.266702 for technical details of the derivation of the overlap elements.
[34] H. Vogt, Refined treatment of the model of linearly coupled anharmonic oscillators and its application to the temperature dependence of the zone-center soft-mode frequencies of $KTaO_3$ and $SrTiO_3$, Phys. Rev. B **51**, 8046 (1995).
[35] K. van Benthem, C. Elsässer, and R. H. French, Bulk electronic structure of $SrTiO_3$: Experiment and theory, J. Appl. Phys. **90**, 6156 (2001).
[36] J.-J. Zhou, O. Hellman, and M. Bernardi, Electron-phonon scattering in the presence of soft modes and electron mobility in $SrTiO_3$ perovskite from first principles, Phys. Rev. Lett. **121**, 226603 (2018).
[37] M. N. Gastiasoro, M. E. Temperini, P. Barone, and J. Lorenzana, Generalized Rashba electron-phonon coupling and superconductivity in strontium titanate, Phys. Rev. Res. **5**, 023177 (2023).
[38] M. Freiser, A survey of magnetooptic effects, IEEE Trans. Magn. **4**, 152 (1968).
[39] D. M. Juraschek, T. C. V. Neuman, and P. Narang, Giant effective magnetic fields from optically driven chiral phonons in $4f$ paramagnets, Phys. Rev. Res. **4**, 013129 (2022).
[40] D. Saparov, B. Xiong, Y. Ren, and Q. Niu, Lattice dynamics with molecular Berry curvature: Chiral optical phonons, Phys. Rev. B **105**, 064303 (2022).